

Stress Intensity Factor using Finite Element Analysis in Rectangular Orthotropic Composite Annular Disk

P. Ravinder Reddy

Chaitanya Bharti Institute of Technology, Hyderabad-500 075.

and

G. Ramamurthy

Osmania University, Hyderabad-500 007.

ABSTRACT

The quadratic isoparametric elements which embody the inverse squareroot singularity were used to determine the stress intensity factor in an annular disk made of Boron-Epoxy composite material. The displacements and stresses were determined in a rectangular orthotropic composite annular disk using isoparametric finite elements. The singularity in the strain field was provided by means of 8-noded isoparametric elements (4-nodes at the four corners and four mid-side nodes each at $1/4^{th}$ distance from the edge). The results were obtained for various material properties and fibre orientation. The geometry of the annular disk was reported when subjected to a boundary radial and tangential load. The r singularity was provided at the boundary of the circular hole and the rest of the annular disk was modelled with ordinary isoparametric elements. The apparent stress intensity factor ($K_I = \sigma \sqrt{r}$) was computed from the stress data near the circular hole, when it was subjected to uniform tension. A curve was drawn for apparent stress intensity factor versus the distance from the crack edge and was extrapolated to $r = 0$, the actual stress intensity factor was found on the y-axis.

NOMENCLATURE

a, b	Outer and inner radii of an annular disk, mm
E_1, E_2	Elastic modulus along fibre direction and perpendicular to fibre direction, GPa
$B = b/a$	Aspect ratio
G_{12}	Shear modulus, GPa
t	Thickness of the disk, mm
θ	Fibre angle
$\sigma_1, \sigma_2, \tau_{12}$	Stresses, in 1-2 direction.

1. INTRODUCTION

In recent years, the increasing use of advanced structural components in aircraft¹⁻³, automobiles, missile systems, and space structures has been well documented. It is therefore important for the structural designers to be familiar with the property of composite materials and their use in designing composite material structures⁴⁻⁵. Some of the most common machine elements like wheels, pulleys, turbine and compressor disks, flywheels⁶, grinding wheels, and other rotating parts can be modelled as a first approximation to annular disks or cylindrical

plates with a circular hole. Flaws and other discontinuities may cause the formation of small cracks, especially in members subjected to repeated loading. To fully utilise the potential of modern highly stressed structures, it is necessary to predict their behaviour in the presence of flaws which frequently exist, more often due to manufacturing/fabrication defects or in-service damage. Successful predictions of service life reduce the need for over-conservative designs, thereby reducing cost and also improving the operational safety of the structures⁷. Since the behaviour of cracks is controlled by strain energy release rates or stress intensity factor of the crack⁸⁻¹⁰, it is necessary to evaluate this for a real structural configuration. Practical problems often arise as a result of the initiation and growth of cracks embedded in an orthotropic composite annular¹¹ disks when subjected to an in-plane load. Damage of this kind will cause the failure.

This paper aims to investigate stress intensity factor in a rectangular orthotropic composite annular disk with a circular hole by the use of isoparametric finite elements.

2. FINITE ELEMENTS IN FRACTURE MECHANICS

The use of finite element method in fracture mechanics has been quite extensive both in the elastic and elastic-plastic range. A number of special crack tip finite elements have been developed¹²⁻¹⁴, using the displacement method and also the hybrid method. These special crack tip elements lack constant strain and rigid body motion modes and as a result they do not pass the patch test and necessary requirements for convergence:

To overcome these problems, the 8-noded isoparametric elements are used (Fig. 1). The singularity in these non-singularity elements is achieved by placing the mid-side nodes near the crack tip at the quarter point. It is well known that such elements in their non-singular formulation satisfy the essential convergence criteria¹⁵, namely, inter-element compatibility, constant strain modes, continuity of displacements, and rigid body motion modes. These elements also pass the patch test.

3. SINGULAR QUADRATIC ISOPARAMETRIC ELEMENTS

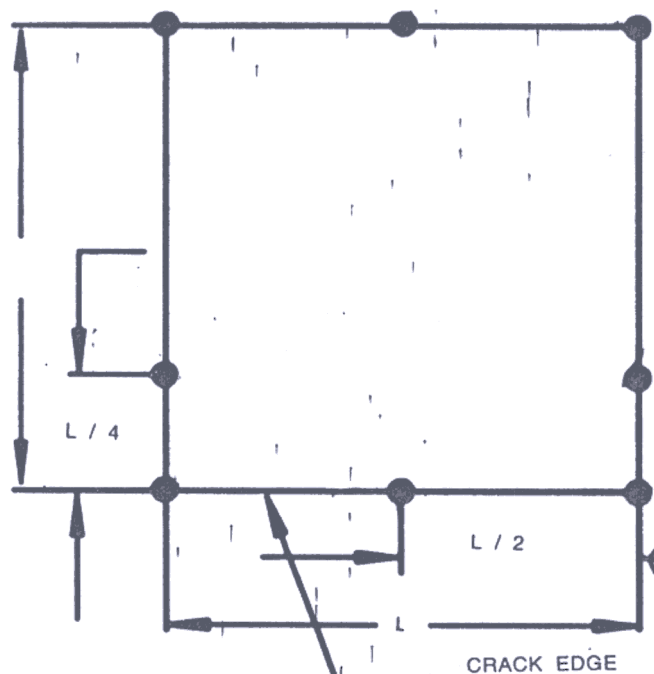


Figure 1. 8-noded isoparametric element with singularity

The formulation of isoparametric element stiffness is well-documented. The geometry of an 8-noded plane isoparametric element is mapped into the normalised square space (ξ, η) $(-1 \leq \xi \leq 1, -1 \leq \eta \leq 1)$ through the following transformations.

$$\begin{aligned} x &= \sum_{i=1}^8 N_i(\xi, \eta) x_i \\ y &= \sum_{i=1}^8 N_i(\xi, \eta) y_i \end{aligned} \quad (1)$$

$$\begin{aligned} N_i &= [(1+\xi \xi_i)(1+\eta \eta_i) - (1-\xi^2)(1+\eta \eta_i) - (1-\eta^2) \\ &\quad [(1+\xi \xi_i)] \xi_i^2 \eta_i^2 / 4 + (1-\xi^2)(1+\eta \eta_i)(1-\xi^2) \eta_i^2 / 2 \\ &\quad + (1-\eta^2)(1+\xi \xi_i)(1-\eta_i^2) \xi_i^2 / 2 \end{aligned}$$

where

N_i are the shape functions corresponding to the node i , whose coordinates are (x_i, y_i) in the x - y system and (ξ_i, η_i) in the transformed ξ, η system.

$(\xi, \eta = +1)$ for corner points and zero for mid-side nodes. The displacements are interpolated by:

$$u = \sum_{i=1}^8 N_i(\xi, \eta) u_i \quad (2)$$

$$v = \sum_{i=1}^8 N_i(\xi, \eta) v_i$$

Strain displacement relationship becomes

$$\{\epsilon\} = [B] \begin{Bmatrix} u_i \\ v_i \end{Bmatrix} \quad (3)$$

where

B is a strain displacement matrix.

$$B = \begin{bmatrix} \frac{\partial N_i}{\partial x} & 0 \\ 0 & \frac{\partial N_i}{\partial y} \\ \frac{\partial N_i}{\partial y} & \frac{\partial N_i}{\partial x} \end{bmatrix} \quad (4)$$

$$\begin{bmatrix} \frac{\partial N_i}{\partial x} \\ \frac{\partial N_i}{\partial y} \end{bmatrix} = [J^{-1}] \begin{bmatrix} \frac{\partial N_i}{\partial \xi} \\ \frac{\partial N_i}{\partial \eta} \end{bmatrix} \quad (5)$$

where

J is the Jacobian matrix and is given by

$$[J] = \begin{bmatrix} \frac{\partial x}{\partial \xi} & \frac{\partial y}{\partial \eta} \\ \frac{\partial x}{\partial \eta} & \frac{\partial y}{\partial \xi} \end{bmatrix} \quad (6)$$

The stress is given by

$$\{\sigma\} = [D] \{\epsilon\} \quad (7)$$

$[D]$ stress-strain matrix, the element stiffness $[K]$ is given by

$$[K] = \int_V [B^T] [D] [B] \det[J] d\xi d\eta \quad (8)$$

To obtain a singular element to be used at the crack tip, the stress equation and the strain equation must be singular. This singularity is achieved by

placing the mid-side node at the quarter points of the sides. For simplicity, the strength of the singularity is found along the line 1-2 ($\eta = -1$) (Fig. 1). The shape functions evaluated along the line 1-2 are

$$\begin{aligned} N_1 &= -1/2 (1 - \xi) \\ N_2 &= 1/2 (1 + \xi) \\ N_5 &= (1 - \xi^2) \end{aligned} \quad (9)$$

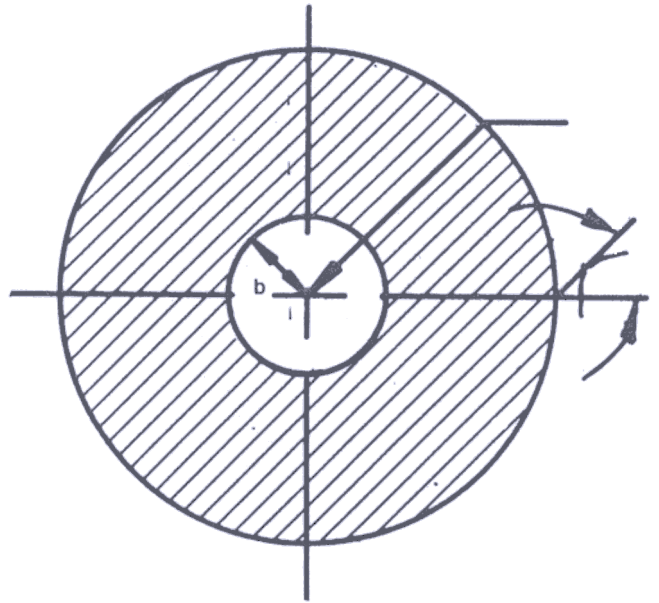


Figure 2. Rectangular orthotropic annular disk

The strain singularity along the line 1-2 is $1/\sqrt{r}$, which is calculated using equations 1 to 9 by substituting position of the nodes.

4. ANALYSIS

4.1 Mesh Generation & Boundary Conditions

Figure 2 shows rectangular orthotropic cylindrical annular disk with a centre hole. The boundary of the circular hole is meshed with 8-noded isoparametric (singular) element. The singularity in this element is achieved by positioning the mid-side node at the quarter point from the crack edge and the rest of the structure is modelled with ordinary 8-noded isoparametric element (i.e four-nodes at the corners and the

remaining four-nodes at mid-sides of the edges). The nodes and the elements incremented radially outward by choosing the smaller size near the circular hole and the larger size at the boundary of the annular disk. The material chosen for the annular disk was Boron/Epoxy and the required boundary conditions were imposed on the model during the analysis.

At the boundary of the annular disk, the concentrated load was applied radially and

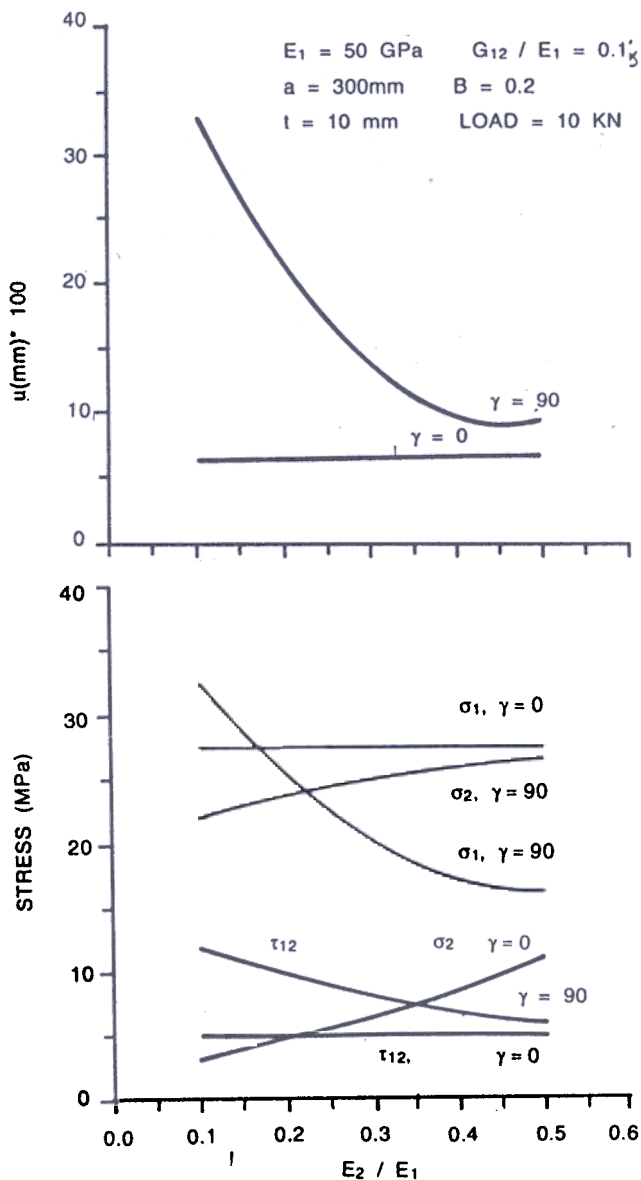


Figure 3. Maximum stresses and displacements vs E_2/E_1 (radial load).

tangentially by varying the fibre orientation, material properties, and aspect ratio, and the results obtained were reported. The stress intensity factor was determined for the circular hole in a rectangular orthotropic annular disk indirectly by computing the stress data near the crack plane.

5. DISCUSSION

5.1 Radial Load

The stress and displacement behaviour of a rectangular orthotropic composite annular disk subjected to a concentrated radial load at the outer edge with respect to various parameters discussed here. Figure 3 shows variation in displacements and stresses with respect to E_2/E_1 . A change of E_2/E_1 causes the minimum deflection to reduce when the fibre angle, $r = 90^\circ$, E_2 is stiffness in the direction of the application of the radial load. Thus, an increase in E_2 is directly responsible for reduction in the maximum deflection in the radial direction. On the other hand, when $r = 0$, E_1 resists the load. σ_1 is dependent to a large extent on the strain in the fibre direction, and E_1 should depend on E_2 and also on the strain in the direction transverse to the fibre direction. Since E_2/E_1 is increased, it can be expected that stresses will increase. Since τ_{12} is dependent on G_{12} and deflections, the reduction in τ_{12} is due to the reduction in deflections which in turn is due to larger stiffness. Figure 4 shows that (i) the deflections reduce for any fibre angle, (ii) maximum stresses in the fibre and transverse direction reduce, and (iii) maximum shear stresses increase with respect to G_{12}/E_1 . This is due to an increase in the stiffness of the annular disk, its influence is less for shear stress. Figure 5 shows the variation of stresses and deflections due to aspect ratio. It is observed that the stresses will increase and deflections reduce as B increases. This is due to the column effect of the annular disk (reduction in length). Figure 6 represents the variation in maximum-induced stresses for various values of fibre orientation. It is observed that σ_1 max. and σ_2 max. exhibit a large change in their magnitudes as r is varied from 0 to 90° . The change in shear

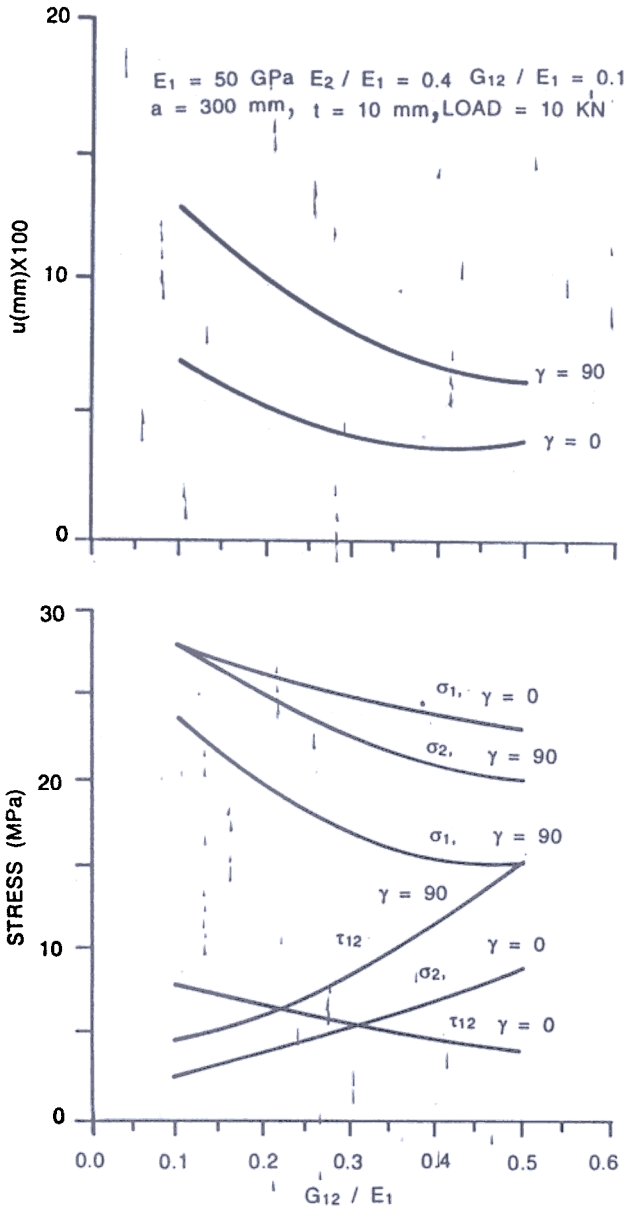


Figure 4. Maximum stresses and displacements vs G_{12}/E_1 (radial load).

stress is also quite large if taken as a percentage of its value at $r = 0$ which would be the most critical in determining the failure.

5.2 Tangential Load

Figure 7 shows the effect of variation in E_2/E_1 on the maximum displacements and stresses in an orthotropic annular disk subjected to a tangential concentrated load at its outer edge. It is observed that the deflection reduces when the fibre angle is

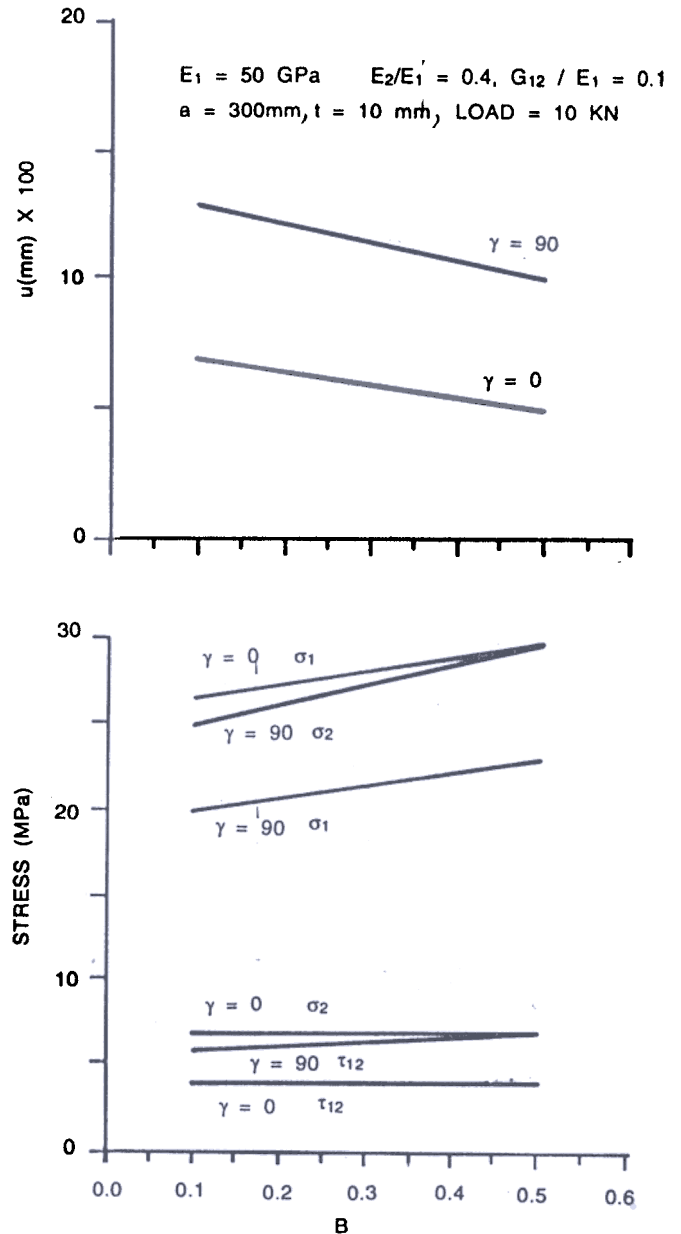


Figure 5. Maximum stresses and displacements vs aspect ratio (radial load).

zero. This is because the strength in the circumferential direction is increased. σ_1 is dependent on the deflection and E_1 , and it reduces due to reduction in displacements. σ_2 depends on E_2 , as E_2/E_1 increases σ_2 also increases and $\tau_{12 \max}$ reduces. Figure 8 shows the maximum displacements and stresses as G_{12}/E_1 is varied. G_{12} plays a major role in determining the deflections. τ_{12} increases and the stresses in the

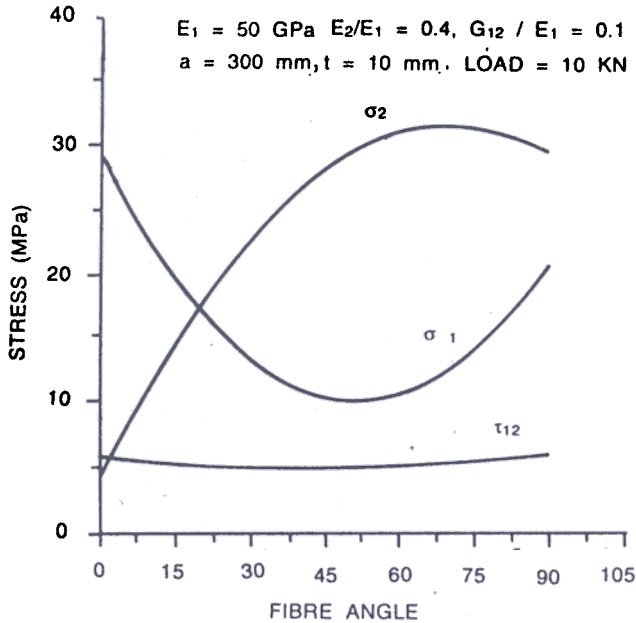


Figure 6. Maximum stresses vs fibre orientation for radial load

fibre direction and also perpendicular to fibre direction reduce due to increase in the value of shear modulus. Figure 9 shows the trends of the maximum displacements and stresses with the variation of aspect ratio, B. When aspect ratio is increased, the width of the annular disk is reduced. This would in-turn reduce the magnitude of the maximum displacement occurring at the point of application of the load. There is a drastic reduction in the maximum displacement when aspect ratio is increased from 0.1 to 0.2. This should be the factor responsible for steep fall in the magnitude of shear stress. Figure 10 shows the variation of stresses by varying the fibre angle. It is observed that the maximum stress in fibre direction and shear stress are increasing whereas the maximum stress perpendicular to fibre direction is reducing when the fibre angle is increased.

6. STRESS INTENSITY FACTOR

When the annular disk is subjected to uniform tension, the stresses surrounding the centre hole are computed. The apparent stress intensity factor is

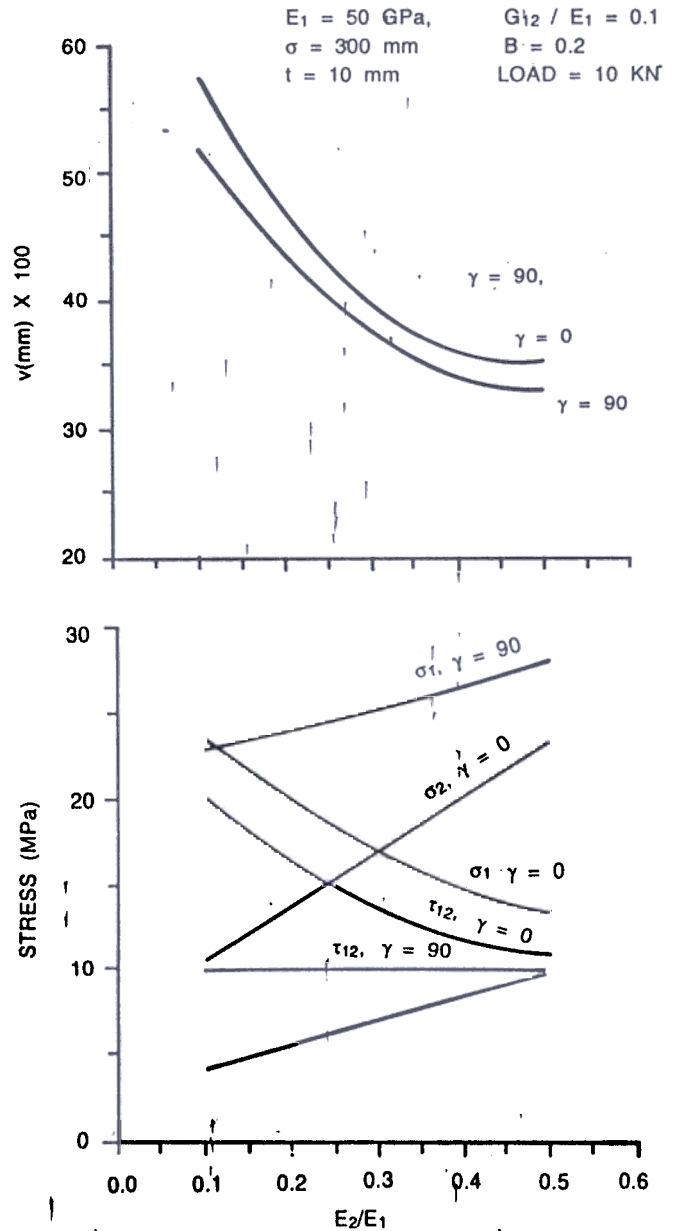


Figure 7. Maximum stresses and displacements vs E_2/E_1 (tangential load).

computed from the computed stress data near the hole. As it is known that the apparent stress intensity factor is r , a curve is drawn for apparent stress intensity factor versus the distance from the crack border (Fig. 11). From the curve, it is observed that as the distance from the crack border increases, the stress intensity factor also increases and the variation becomes linear. The linear part of

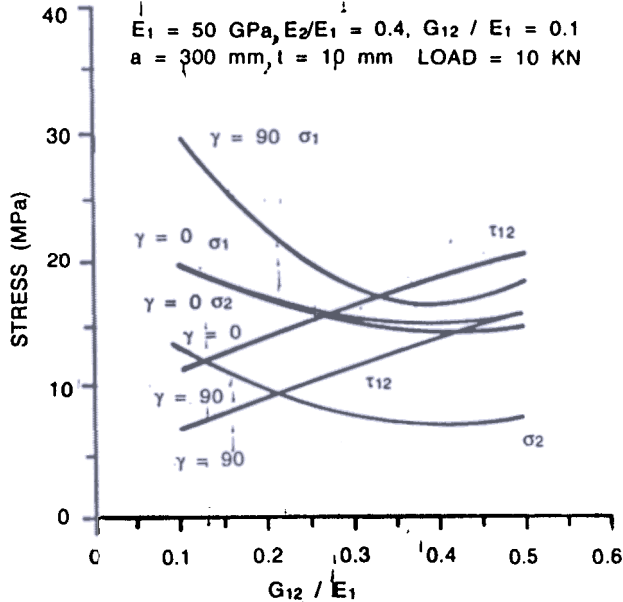
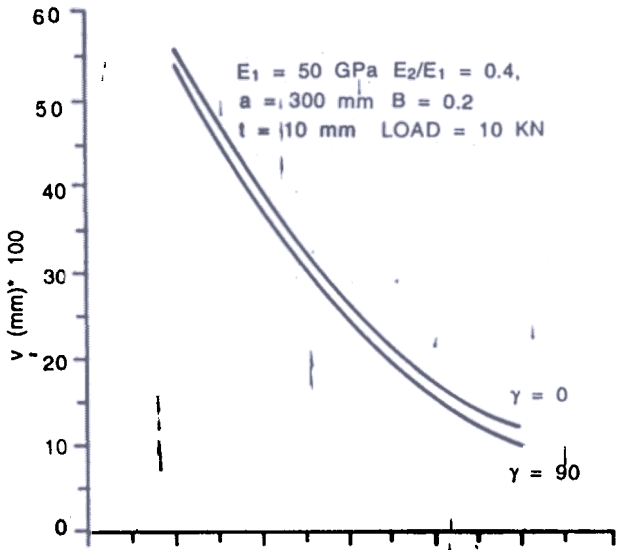


Figure 8. Maximum stresses and displacements vs G_{12}/E_1 (tangential load).

the curve is extrapolated to $r = 0$, the actual stress intensity factor is determined as $150^{-3/2} \text{ N-mm}$.

7. CONCLUSIONS

From the results obtained in the annular disk analysis, the following conclusions are drawn:

1. The variation in the stresses depend on the orthotropic constants. The constant, which is

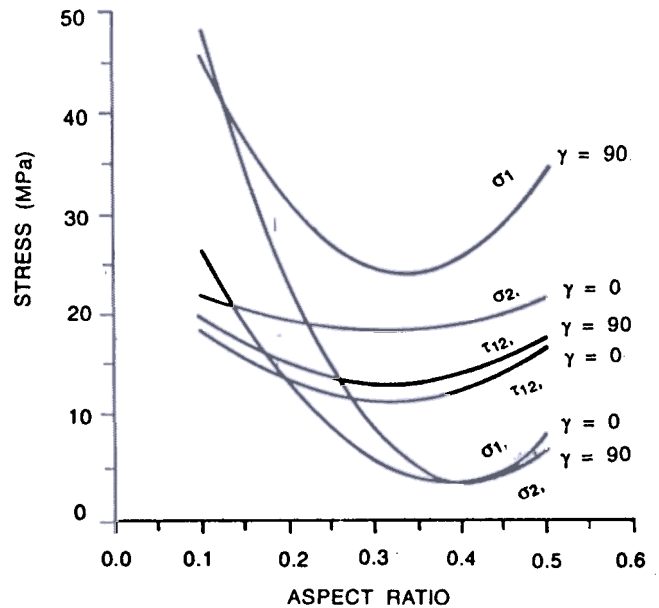
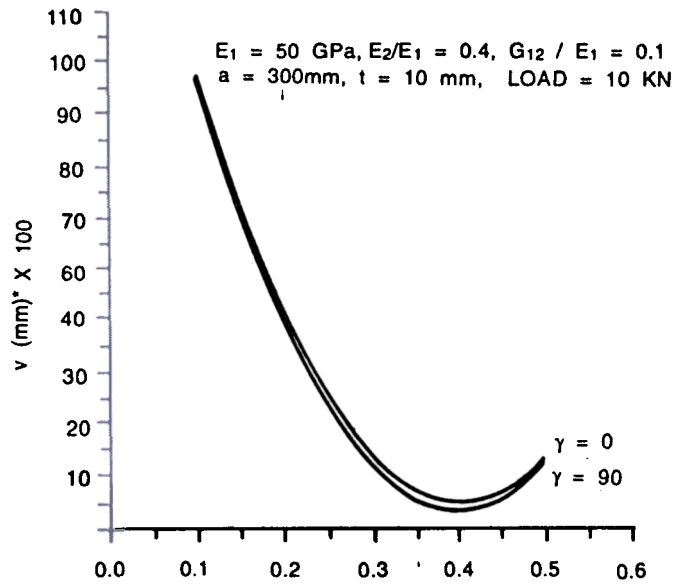


Figure 9. Maximum stresses and displacements vs aspect ratio (tangential load).

varying has an influence on the computed stresses in the annular disk.

2. Stress intensity factor is determined indirectly from the computed stress data near the circular hole and the procedure can be extended for any material, geometry of the crack and the type of the load.

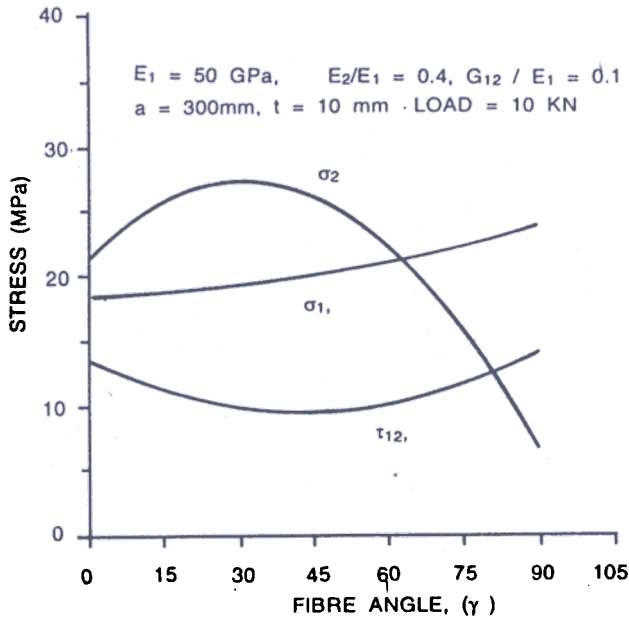


Figure 10. Maximum stresses vs fibre angle (tangential load)

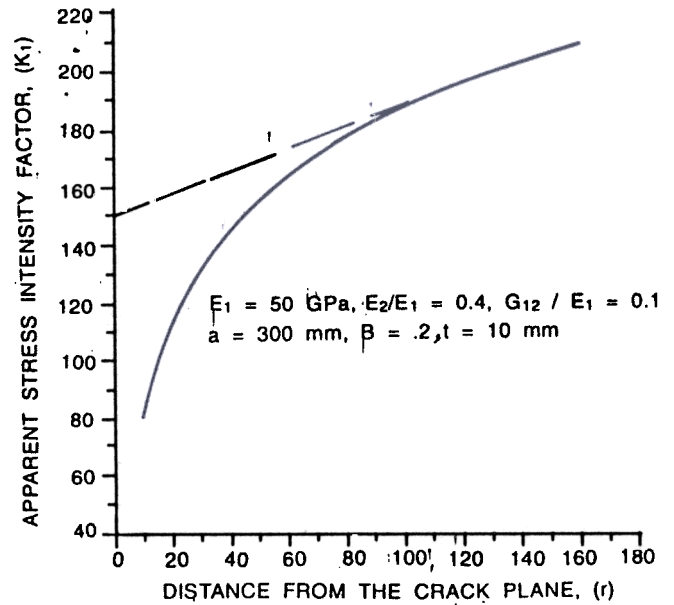


Figure 11. Apparent stress intensity factor vs distance from the crack plane, r.

REFERENCES

1. Way, S. A laterally loaded clamped square plate with large deformations. Paper presented at the 5th International Conference on Applied Mechanics. Wiley, New York, 1988, pp. 123-38.
2. Reddy, J.N. A generalisation of two-dimensional theories of laminated composite plates. *Commun. Applied Numer. Methods*, 1987, 3, 113-80.
3. Rao, G.V. et al. A study of various effects on the stability of circular plates. *Computational Structures*, 1986, 24, 39-45.
4. Jones, R.M. Mechanics of composite materials. Mc-Graw Hill, New York, 1975.
5. James, M.W. & Issac, M.D. Experimental mechanics of fibre reinforced composites materials. Prentice-Hall, 1980.
6. Suzuki, Y. et al. A study of molding method and strength of fibre reinforced plastic gear. *Bull. JSME*, 1981, 24, 2177-83.
7. Barsoum, R.S. On the use of isoparametric finite elements in linear fracture mechanics. *Int. J. Num. Methods Engg.*, 1976, 10, 35-57.
8. Tracey, D.M. 3-D elastic singularity element for evaluation of K along arbitrary crack front. *Int. J. Fract.*, 1971, 7, 340-43.
9. Byskov, E. The calculation of stress intensity factors using the finite element method with cracked elements. *Int. J. Fract.*, 1970, 6, 159-67.
10. Tracey, D.M. Finite element for determination of crack tip elastic stress intensity factors. *Engg. Fract. Mech.*, 1970, 2, 159-67.
11. Ravinder Reddy, P.; Reddy, P.R.K.; Chamundeshwari, K. & Sridevi, D. Stress intensity factor in cylindrically orthotropic composite plates with a circular hole. Proceedings of the IX th ISME Conference, 10-11 November 94, University of Roorkee.
12. Benzley, S.E. Representation of singularities with isoparametric finite elements. *Int. J. Num. Methods. Engg.*, 1974, 8, 537-45.
13. Chan, S.K.; Tuba, I.S. & Wilson, W.K. On the finite element method in linear fracture mechanics. *Engg. Fract. Mech.*, 1970, 2, 1-17.

14. Anderson, G.P.; Ruggles. & Seibor, G.S. Use of finite element computer programs in fracture mechanics. *Int. J. Fract. Mech.*, 1971, 7, 63-76.
15. Zienkiewicz, O.C. The finite element method in engineering science. Mc-Graw Hill, London, 1971.

Contributor



Mr P Ravinder Reddy is in-charge of CAD/CAM Centre, Mechanical Engineering Department, Chaitanya Bharti Institute of Technology, Hyderabad. He received his BTech and ME in Mechanical Engineering, from Kakatiya University. Presently, he is doing his PhD in Computer-Aided Engineering and Analysis of FRP & MM Composites from Osmania University, Hyderabad. He has guided 10 MTech theses in CAD/CAM, FEA, Expert Systems and AI, and Advanced Materials. He has published 20 papers in national/international journals and conferences.